Phosphine Addition and Substitution Reactions on Unusually Reactive Triosmium Clusters: $(\mu\text{-H})(\mu_3\text{-}\eta^2\text{-C=NCH}_2\text{CH}_2\text{CH}_2)\text{Os}_3(\text{CO})_9$ and $(\mu\text{-H})(\mu_3\text{-}\eta^2\text{-CH}_3\text{CH}_2\text{C=NCH}_2\text{CH}_2\text{CH}_3)\text{Os}_3(\text{CO})_9$

Michael Day, David Espitia, Kenneth I. Hardcastle, Shariff E. Kabir, and Edward Rosenberg*

Department of Chemistry, California State University, Northridge, California 91330

Roberto Gobetto, Luciano Milone,* and Domenico Osella

Dipartimento di Chimica Inorganica, Chimica Fisica e Chimica dei Materiali,
Università di Torino, Via Giuria 7-9, I 10125 Torino, Italy

Received April 4, 1991

The reactions of $(\mu\text{-H})(\mu_3\text{-}\eta^2\text{-C=NCH}_2\text{CH}_2\text{CH}_2)\text{Os}_3(\text{CO})_9$ (**1**), $(\mu\text{-H})(\mu_3\text{-}\eta^2\text{-CH}_3\text{CH}_2\text{C=NCH}_2\text{CH}_2\text{CH}_3)\text{Os}_3(\text{CO})_9$ (**2**), $(\mu\text{-H})(\mu\text{-}\eta^2\text{-C=NCH}_2\text{CH}_2\text{CH}_2)\text{Os}_3(\text{CO})_{10}$ (**3**), and $(\mu\text{-H})(\mu\text{-}\eta^2\text{-CH}_3\text{CH}_2\text{C=NCH}_2\text{CH}_2\text{CH}_3)\text{Os}_3(\text{CO})_{10}$ (**4**) with trialkylphosphines at 25–100 °C have been studied. At room temperature **1** gives a phosphine addition product $(\mu\text{-H})(\mu\text{-}\eta^2\text{-C=NCH}_2\text{CH}_2\text{CH}_2)\text{Os}_3(\text{CO})_9\text{P}(\text{C}_6\text{H}_5)_3$ (**5**) where the phosphine has added to the metal atom formerly π-bound to the C=N bond of the μ_3-imidoyl ligand; **5** exists as two isomers in solution. Compound **5** rearranges to the isomeric **6a** and **6b** at 100 °C in which the phosphine is at one of the two metal atoms bridged by the hydride and the imidoyl ligand. At 100 °C **3** substitutes phosphine for carbonyl to also give **6a** and **6b**, which on further thermolysis at 125 °C decarbonylate to give $(\mu\text{-H})(\mu_3\text{-}\eta^2\text{-C=NCH}_2\text{CH}_2\text{CH}_2)\text{Os}_3(\text{CO})_8\text{P}(\text{C}_6\text{H}_5)_3$ (**7**). In contrast, reaction of **2** with triphenylphosphine at room temperature gives $(\mu\text{-H})(\mu\text{-}\eta^2\text{-CH}_3\text{CH}_2\text{C=NCH}_2\text{CH}_2\text{CH}_3)\text{Os}_3(\text{CO})_9\text{P}(\text{C}_6\text{H}_5)_3)$ (**8**), which exists as a mixture of five of six possible positional isomers with respect to location of the phosphine, hydride, and imidoyl ligands in solution. The reaction of **4** with triphenylphosphine at 100 °C gives this same mixture of isomers. Decarbonylation of **8** proceeds at 125 °C to give $(\mu\text{-H})(\mu_3\text{-}\eta^2\text{-CH}_3\text{CH}_2\text{C=NCH}_2\text{CH}_2\text{CH}_3)\text{Os}_3(\text{CO})_8\text{P}(\text{C}_6\text{H}_5)_3)$ (**9**) and the dihydrido orthometalation product $(\mu\text{-H})_2(\mu\text{-}\eta^2\text{-CH}_3\text{CH}_2\text{C=NCH}_2\text{CH}_2\text{CH}_3)\text{Os}_3(\text{CO})_8(\mu\text{-}\eta^2\text{-}(\text{C}_6\text{H}_5)_2\text{P}(o\text{-C}_6\text{H}_4))$ (**10**). Reaction of **2** with trimethylphosphine or trimethyl phosphite gives the addition products $(\mu\text{-H})(\mu\text{-}\eta^2\text{-CH}_3\text{CH}_2\text{C=NCH}_2\text{CH}_2\text{CH}_3)\text{Os}_3(\text{CO})_9\text{PR}_3$ ($\text{R} = \text{CH}_3$, **11**; $\text{R} = \text{OCH}_3$, **12**), which are structurally analogous to **5** in solution. The origin of the structural differences between the addition products obtained from the reaction of **1** and **2** with $\text{P}(\text{C}_6\text{H}_5)_3$ and from **2** with the different phosphorous ligands is discussed in terms of steric interactions between the imidoyl ligand and the phosphorous ligand. All compounds reported were characterized by ^{1}H NMR, infrared spectroscopy, and elemental analysis. In addition, solid-state structures for **5**, **6a**, **8a**, and **9** were determined. Compound **5** crystallizes in the triclinic space group $P\bar{1}$ (No. 2) with unit cell parameters $a = 10.762$ (2) Å, $b = 17.442$ (2) Å, $c = 8.595$ (2) Å, $\alpha = 97.38$ (1)°, $\beta = 94.04$ (1)°, $\gamma = 97.44$ (1)°, $V = 1580$ (1) Å^3, and $Z = 2$. Subsequent least-squares refinement of 5058 reflections gave a final agreement factor of $R = 0.032$ ($R_w = 0.041$). Compound **6a** crystallizes in the monoclinic space group $P2_1/c$ (No. 14) with unit cell parameters $a = 9.307$ (2) Å, $b = 15.601$ (3) Å, $c = 21.773$ (4) Å, $\beta = 97.59$ (2)°, $V = 3134$ (2) Å^3, and $Z = 4$. Least-squares refinement of 4316 reflections gave a final agreement factor of $R = 0.029$ ($R_w = 0.036$). Compound **8a** crystallizes in the triclinic space group $P\bar{1}$ (No. 2) with unit cell parameters $a = 12.684$ (3) Å, $b = 16.254$ (3) Å, $c = 9.561$ (2) Å, $\alpha = 99.53$ (1)°, $\beta = 96.69$ (2)°, $\gamma = 112.57$ (2) Å, $V = 1760$ (1) Å^3, and $Z = 2$. Least-squares refinement of 4236 reflections gave a final agreement factor of $R = 0.031$ ($R_w = 0.038$). Compound **9** crystallizes in the orthorhombic space group $P2_12_12_1$ (No. 19) with unit cell parameters $a = 9.626$ (1) Å, $b = 15.342$ (2) Å, $c = 22.849$ (3) Å, $V = 3374$ (1) Å^3, and $Z = 4$. Least-squares refinement of 2841 reflections gave a final agreement factor of $R = 0.031$ ($R_w = 0.027$).

Introduction

Ligand substitution reactions on valence-saturated osmium carbonyl clusters normally take place at elevated temperatures.[1-3] Although these substitution reactions often exhibit an associative component in their rate laws and can occur with activation energies below that required for carbonyl–metal bond cleavage, the dissociation of a carbonyl ligand is always part of the rate-determining process.[3b] Recently, there have been several reports in the literature of valence-saturated trinuclear clusters undergoing ligand addition and substitution reactions with phosphines and other two-electron donors at or below room temperature.[4-7] These reactions are usually associated with cleavage of a metal–metal bond (often reversible) or

---

[1] (1) Deeming, A. J.; Johnson, B. F. G.; Lewis, J. *J. Chem. Soc. A* **1970**, 897. Deeming, A. J.; Underhil, M. *J. Chem. Soc., Dalton Trans.* **1973**, 2727; Deeming, A. J.; Kimber, R. E.; Underhill, M. *J. Chem. Soc., Dalton Trans.* **1973**, 2589.

[2] (2) Shojaie, A.; Atwood, J. D. *Organometallics* **1985**, *4*, 187.

[3] (3) Poe, A. J.; Twigg, J. *J. Chem. Soc., Dalton Trans.* **1974**, 1860. Poe, A. J.; Sekhar, V. C. *Inorg. Chem.* **1985**, *24*, 4376.

[4] (4) (a) Huttner, G.; Knoll, K. *Angew. Chem., Int. Ed. Engl.* **1987**, *26*, 743 and references therein. (b) Carty, A. J.; MacLaughlin, S. A.; Taylor, N. J. *J. Organomet. Chem.* **1981**, *204*, C 27. (c) Planalp, R. P.; Vahrenkamp, H. *Organometallics* **1987**, *6*, 492.

[5] (5) Deeming, A. J.; Donovan-Mtunzi, S.; Kabir, S. E.; Manning, P. J. *J. Chem. Soc., Dalton Trans.* **1985**, 1037.

[6] (6) (a) Mayr, A.; Lin, Y. C.; Boag, N. M.; Kampe, C. E.; Knobler, C. B.; Kaesz, H. D. *Inorg. Chem.* **1984**, *23*, 4646. (b) Keijsper, J.; Polm, L. H.; van Koten, G.; Vrieze, K.; Seignette, P. F. A.; Stam, C. H. *Inorg. Chem.* **1985**, *24*, 518. (c) Adams, R. D.; Golembeski, N. M. *J. Am. Chem. Soc.* **1979**, *101*, 2579. (d) Adams, R. D.; Katahira, D. A.; Wang, L. W. *J. Organomet. Chem.* **1981**, *219*, 85.

[7] (7) (a) Lugan, N.; Lavigne, G.; Bonnet, J. *J. Inorg. Chem.* **1987**, *26*, 585. (b) Lugan, N.; Lavigne, G.; Bonnet, J. J.; Reau, R.; Neibecker, D.; Tkatchenko, I. *J. Am. Chem. Soc.* **1988**, *110*, 5369.

0276-7333/91/2310-3550$02.50/0

the presence of a mobile[7] or cis-labilizing ligand.[4] We have recently synthesized a range of trinuclear clusters of osmium and ruthenium with face-capping nitrogen-containing ligands that exhibit unusually high reactivity toward ligand addition and substitution reactions.[8] We report here the details of our studies of the reactions of phosphines with the triosmium clusters $(\mu\text{-H})(\mu_3\text{-}\eta^2\text{-}\overline{\mathrm{C{=}NCH_2CH_2C}}\mathrm{H_2})\mathrm{Os_3(CO)_9}$ (1) and $(\mu\text{-H})(\mu_3\text{-}\eta^2\text{-}\mathrm{CH_3CH_2C{=}NCH_2CH_2CH_3})\mathrm{Os_3(CO)_9}$ (2), which are obtained in good yields from decarbonylation of $(\mu\text{-H})(\mu\text{-}\eta^2\text{-}\overline{\mathrm{C{=}NCH_2CH_2C}}\mathrm{H_2})\mathrm{Os_3(CO)_{10}}$ (3) and $(\mu\text{-H})(\mu\text{-}\eta^2\text{-}\mathrm{CH_3CH_2C{=}NCH_2CH_2CH_3})\mathrm{Os_3(CO)_{10}}$ (4), which are in turn synthesized from the reactions of pyrrolidine and di-*n*-propylamine with $\mathrm{Os_3(CO)_{10}(CH_3CN)_2}$, respectively (eqs 1 and 2).

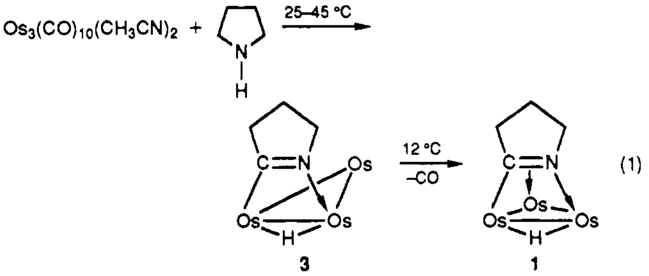

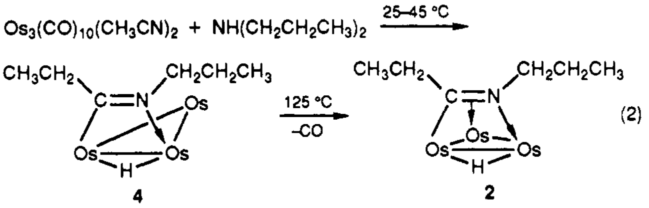

We have not only observed room temperature ligand addition for 1 and 2 but also a remarkable sensitivity toward the product obtained, depending on the structure of amine ligands and the steric bulk of the phosphine ligands.

Results and Discussion

The reaction of 1 with triphenylphosphine at room temperature leads to gradual conversion to the addition product $(\mu\text{-H})(\mu\text{-}\eta^2\text{-}\overline{\mathrm{C{=}NCH_2CH_2C}}\mathrm{H_2})\mathrm{Os_3(CO)_9P(C_6H_5)_3}$ (5) in 93% yield (eq 3). The structure of 5 can be partially inferred from the ^{1}H NMR data alone, which exhibits a slightly broadened singlet hydride resonance at −15.04 ppm. At low temperature (−50 °C) the broadened singlet is resolved into two sharp singlets at −15.01 and −15.08 ppm with a relative intensity of 1:2. We interpret these results as being due to the existence of two radial isomers in solution with the phosphine substituted on the unbridged osmium atom whose interconversion by the usual trigonal twist mechanism is rapid on the ^{1}H NMR time scale at room temperature (Scheme I).

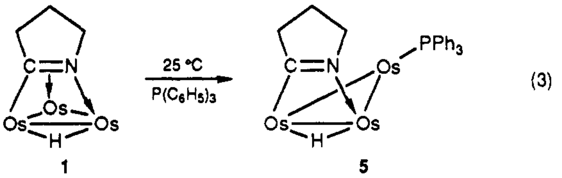

Scheme I

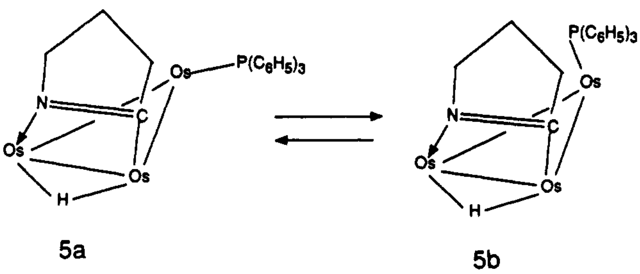

Table I. Crystal Data: Collection and Refinement Parameters

	compound			
	5	**6a**	**8a**	**9**
formula	$C_{31}H_{22}NO_9$-POs_3	$C_{31}H_{22}NO_9$-POs_3	$C_{33}H_{28}NO_9$-POs_3	$C_{32}H_{28}NO_8$-POs_3
fw	1154.10	1154.10	1184.17	1156.16
cryst syst	triclinic	monoclinic	triclinic	orthorhombic
space group	$P\bar{1}$	$P2_1/c$	$P\bar{1}$	$P2_12_12_1$
a, Å	10.762 (2)	9.307 (2)	12.684 (3)	9.626 (1)
b, Å	17.442 (2)	15.601 (3)	16.254 (3)	15.342 (2)
c, Å	8.595 (2)	21.773 (4)	9.561 (2)	22.849 (3)
α, deg	97.38 (1)		99.53 (1)	
β, deg	94.04 (1)	97.59 (2)	96.69 (2)	
γ, deg	97.44 (1)		112.57 (2)	
V, Å^3	1580	3134	1760	3374
Z	2	4	2	4
density$_{\mathrm{calc}}$, g/cm^3	2.43	2.45	2.23	2.28
abs coeff, μ, cm^{-1}	121.6	122.6	109.2	113.8
data collect temp, °C	25 ± 1	25 ± 1	25 ± 1	25 ± 1
radiatn	Mo Kα	Mo Kα	Mo Kα	Mo Kα
scan mode	ω–2θ	ω–2θ	ω–2θ	ω–2θ
scan limits, deg	$4 < 2\theta <$ 50°	$4 < 2\theta <$ 48	$4 < 2\theta <$ 48	$4 < 2\theta <$ 56
scan speed, deg/min	7.2–8.2	7.2–8.2	7.2–8.2	7.2–8.2
scan range, deg	0.8	0.8	0.8	0.8
no. of data	5537	5125	5496	4574
no. obsd	5058	4316	4236	2841
no. variables	406	406	424	406
R^a	0.032	0.029	0.031	0.031^c
$R_w{}^b$	0.041	0.036	0.038	0.027
largest shift/esd	0.0	0.0	0.0	0.0
weighting scheme	$1/\sigma^2$	$1/\sigma^2$	$1/\sigma^2$	$1/\sigma^2$
highest peak in final diff map, e Å^{-3}	1.04 (23)	0.58 (20)	0.74 (21)	0.67 (16)
rel transmissn coeff	0.26–1.00	0.72–1.00	0.31–1.00	0.76–1.00

$^a R = \sum(|F_0| - |F_c|)/\sum|F_0|$. $^b R_w = [(\sum w(|F_0| - |F_c|)^2/\sum w|F_0|^2]^{1/2}$. ^{c}The enantiomer of 9 gave the following convergence results: R, 0.0308; R_w, 0.0261; GOF, 0.97.

At an $\mathrm{Os(CO)_3L}$ center such a trigonal twist involves simultaneous motion of three of the four ligands with one axial ligand remaining stationary. Alternation of the axial ligand involved in this process ultimately exchanges all sites.[10] We have previously shown that phosphine ligands in related triruthenium clusters can participate in a trigonal twist with two other carbonyl ligands.[11] Phosphorus–hydrogen coupling constants between hydrides and phosphine on the same metal atom are usually in the range

---

[8] (a) Rosenberg, E.; Kabir, S. E.; Hardcastle, K. I.; Day, M.; Wolf, E. *Organometallics* **1990**, *9*, 2214. (b) Rosenberg, E.; Hardcastle, K. I.; Day, M.; Hajela, S.; Wolf, E.; Molone, L.; Geobetto, R. Abstracts, 1989 Pacifichem Meeting, Honolulu, HI, Dec 17–22; American Chemical Society: Washington, DC, 1989. (c) Day, M. W.; Hajela, S.; Kabir, S. E.; Irving, M.; McPhillips, T.; Wolf, E.; Hardcastle, K. I.; Rosenberg, E.; Gobetto, R.; Milone, L.; Osella, D. *Organometallics*, in press.

[9] Deeming, A. J.; Donovan-Mtunzi, S.; Kabir, S. E.; Hursthouse, M. B.; Malik, K. M. A.; Walker, N. P. C. *J. Chem. Soc., Dalton Trans.* **1987**, 1869. (b) Deeming, A. J.; Hardcastle, K. I.; Kabir, S. E. *J. Chem. Soc., Dalton Trans.* **1988**, 827. (c) Feighery, W. G.; Allendoerfer, R. D.; Keister, J. B. *Organometallics* **1990**, *9*, 2424. (d) Raithby, P. R. *J. Chem. Soc., Dalton Trans.* **1987**, 931.

[10] Bryan, E. G.; Forster, A.; Johnson, B. F. G.; Lewis, J.; Matheson, T. W. *J. Chem. Soc., Dalton Trans.* **1978**, 196.

[11] Rosenberg, E.; Barner, C.; Milone, L.; Aime, S. *Inorg. Chem.* **1985**, *24*, 231.

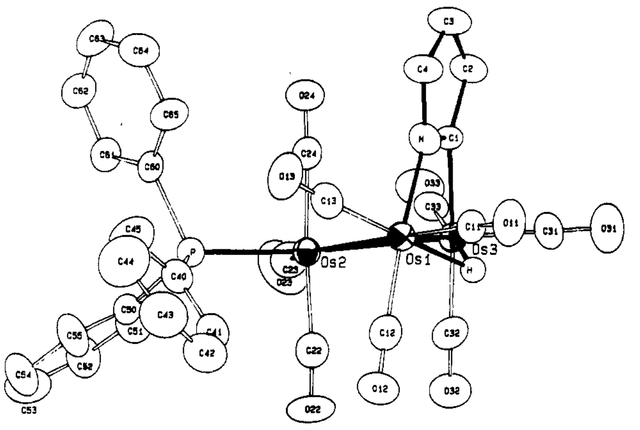

Figure 1. ORTEP drawing of $(\mu\text{-H})(\mu\text{-}\eta^2\text{-}\overline{\mathrm{C{=}NCH_2CH_2CH_2}})\mathrm{Os_3(CO)_9P(C_6H_5)_3}$ (**5**) showing the calculated position of the hydride.

Table II. Selected Bond Distances and Angles for $(\mu\text{-H})(\mu\text{-}\eta^2\text{-}\overline{\mathrm{C{=}NCH_2CH_2CH_2}})\mathrm{Os_3(CO)_9P(C_6H_5)_3}$ (5)[a]

atom 1	atom 2	dist, Å	atom 1	atom 2	dist, Å
Os1	Os2	2.9115 (4)	N	C1	1.275 (8)
Os1	Os3	2.9207 (4)	N	C4	1.50 (1)
Os2	Os3	2.8917 (4)	C1	C2	1.48 (1)
Os1	N	2.093 (7)	C2	C3	1.53 (1)
Os2	P	2.371 (2)	C3	C4	1.56 (1)
Os3	C1	2.107 (7)	C	O(CO)	1.14 (1)[b]
Os1	H	1.85	P	C(Ph)	1.85 (3)[b]
Os3	H	1.85	C	C(Ph)	1.39 (2)[b]
Os	C(CO)	1.90 (2)[b]			

atom 1	atom 2	atom 3	angle, deg	atom 1	atom 2	atom 3	angle, deg
Os2	Os1	Os3	59.448 (9)	Os2	P	C40	116.9 (3)
Os1	Os3	Os2	60.118 (9)	Os2	P	C50	117.7 (3)
Os1	Os2	Os3	60.434 (9)	Os2	P	C60	111.6 (2)
C1	N	C4	113.0 (6)	C40	P	C50	102.1 (4)
N	C1	C2	113.8 (6)	C40	P	C60	104.9 (4)
C1	C2	C3	104.6 (6)	C50	P	C60	101.8 (4)
C2	C3	C4	105.5 (6)	Os	C	O(CO)	176 (2)[b]
N	C4	C3	103.0 (6)	C	C	C(Ph)	120 (2)[b]

[a] Numbers in parentheses are estimated standard deviations in the least significant digits. [b] Average values.

7-15 Hz.[9] At +50 °C the slightly broadened hydride resonance becomes sharper. Although the ^{1}H NMR data indicate the relationship between the hydride ligand and the phosphine, we could not be certain that the relationship between the hydride and the organic ligand is the same in **5** as in **1** and **3**. We therefore undertook a solid-state structural investigation of **5**.

The solid-state structure of **5** is shown in Figure 1, crystal data are in Table I, and selected distances and bond angles are given in Table II. As indicated from the observation of a singlet resonance for the hydride in the ^{1}H NMR, the phosphine has added to the unbridged osmium atom Os(2) and occupies an equatorial position on this atom along with three carbonyl groups. The overall structure of **5** is virtually identical with the previously reported $(\mu\text{-H})(\mu\text{-}\eta^2\text{-}\overline{\mathrm{C{=}NCH_2CH_2CH_2}})\mathrm{Os_3(CO)_{10}}$ (**3**),[8a] with only slight elongations in the Os(1)-Os(2) and Os(2)-Os(3) bonds [2.91 (1) and 2.89 (1) Å in **5** and 2.87 (1) and 2.78 (1) Å in **3**]. Interestingly, phosphine substitution at the remote metal atom causes a significant shortening of the metal-carbon and metal-nitrogen bonds of the imidoyl ligand [Os(1)-N = 2.09 (1) Å, Os(3)-C(1) = 2.11 (1) Å in **5**; Os(1)-N = 2.12 (1) Å, Os(3)-C = 2.14 (1) Å in **3**]. The hydride was located by using the program Hydex.[12]

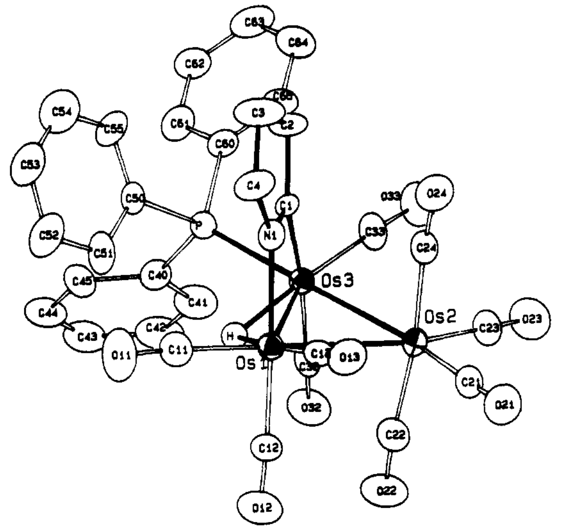

Figure 2. ORTEP drawing of $(\mu\text{-H})(\mu\text{-}\eta^2\text{-}\overline{\mathrm{C{=}NCH_2CH_2CH_2}})\mathrm{Os_3(CO)_9P(C_6H_5)_3}$ (**6a**) showing the calculated position of the hydride ligand.

In the solid-state structure the phosphine is syn to the nitrogen atom of the imidoyl ligand, suggesting that this is the major isomer in solution (Scheme I).

Thermolysis of **5** in refluxing heptane leads to isomerization giving compounds **6a** and **6b** (eq 4) in a ratio of 4:1, where the phosphine is now substituted at osmium atoms bound to the bridging hydride. The equal and relatively large size of the phosphorus-hydrogen coupling[9] (9.9 Hz in **6a** and 10.0 Hz in **6b**) observed for the hydride resonances in both isomers suggests that the phosphine occupies stereochemically similar positions relative to the hydride and therefore probably differ by substitution at the carbon-bound osmium atom (**6a**) versus the nitrogen-bound osmium atom (**6b**, eq 4). As for **5** we could not be certain of the disposition of the organic ligand relative to the phosphine and an X-ray structure determination of the single crystals isolated from this isomeric mixture was undertaken.

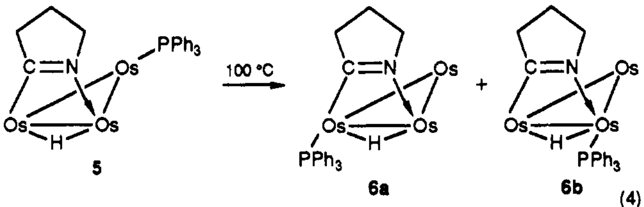

(4)

The solid-state structure of the isomerization product from **5** revealed it to indeed have the structure proposed for **6a** with the phosphine cisoid to the hydride and on the same osmium bound to the carbon of the imidoyl ligand. The structure of **6a** is shown in Figure 2, crystal data are in Table I, and selected distances and bond angles are given in Table III. Again, as for **5**, the metal-metal bonds to the phosphine-substituted metal atom in **6a** are slightly elongated relative to the same bonds in **3** [Os(1)-Os(2) = 2.87 (1) Å, Os(1)-Os(3) = 2.95 (1) Å in **6a**, and Os(1)-Os(2) = 2.78 (1) Å, Os(1)-Os(3) = 2.87 (1) Å in **3**], while the Os(1)-C and Os(3)-N bonds are intermediate in length between those of **5** and **3**. The position of the hydride ligand was calculated by the program Hydex.[12] We assume that **6a** is the major isomer in solution. Two structures directly analogous to **6a** have been reported by Adams et al.: $(\mu\text{-H})(\mu\text{-}\eta^2\text{-C_6H_5N{=}CH})\mathrm{Os_3(CO)_9(P(OCH_3)_3)}$[6c] and $(\mu\text{-H})(\mu\text{-}\eta^2\text{-CF_3C{=}NH})\mathrm{Os_3(CO)_9(P(CH_3)_2C_6H_5)}$,[6d] obtained by reaction of $(\mu\text{-H})(\mu_3\text{-}\eta^2\text{-C_6H_5C{=}N})\mathrm{Os_3(CO)_9}$ with P(O-

---

[12] Orpen, A. G. *J. Chem. Soc., Dalton Trans.* **1980**, 2509.

Table III. Selected Bond Distances and Angles for $(\mu\text{-H})(\mu\text{-}\eta^2\text{-}\overline{C{=}NCH_2CH_2CH_2})Os_3(CO)_9P(C_6H_5)_3$ (6a)[a]

atom 1	atom 2	dist, Å	atom 1	atom 2	dist, Å
Os1	Os2	2.8658 (4)	N1	C1	1.29 (1)
Os1	Os3	2.9496 (5)	N1	C4	1.49 (1)
Os2	Os3	2.8849 (5)	C1	C2	1.54 (1)
Os1	N1	2.094 (7)	C2	C3	1.56 (1)
Os3	C1	2.105 (7)	C3	C4	1.53 (1)
Os3	P	2.354 (2)	C	O(CO)	1.13 (1)[b]
Os1	H	1.85	P	C(Ph)	1.84 (3)[b]
Os3	H	1.85	C	C(Ph)	1.40 (2)[b]
Os	C(CO)	1.91 (2)[b]			

atom 1	atom 2	atom 3	angle, deg	atom 1	atom 2	atom 3	angle, deg
Os1	Os2	Os3	61.72 (1)	Os3	P	C40	118.0 (3)
Os1	Os3	Os2	58.82 (1)	Os3	P	C50	113.0 (3)
Os2	Os1	Os3	59.46 (1)	Os3	P	C60	116.3 (2)
N1	C1	C2	110.1 (7)	C40	P	C50	104.2 (4)
C1	C2	C3	103.5 (7)	C40	P	C60	99.7 (4)
C2	C3	C4	106.4 (7)	C50	P	C60	103.6 (4)
N1	C4	C3	103.5 (7)	Os	C	O(CO)	177 (2)[b]
C1	N1	C4	115.7 (7)	C	C	C(Ph)	120 (1)[b]

[a] Numbers in parentheses are estimated standard deviations in the least significant digits. [b] Average values.

$CH_3)_3$ and of $(\mu\text{-H})_2Os_3(CO)_9(P(CH_3)_2C_6H_5)$ with CF_3CN, respectively. The trimethyl phosphite is substituted under the carbon atom of the imidoyl ligand, whereas the dimethylphenylphosphine is substituted under the nitrogen atom of the imidoyl ligand. Interestingly, these authors did not report the isolation of products related to 5, suggesting that isolation of an initial adduct like 5 from room temperature reactions of phosphines with μ_3-imidoyl ligand clusters is dependent on the structure of the imidoyl ligand and of the phosphorous ligand (vide infra). The observed isomerization of 5 to **6a** and **6b** can be explained by an intramolecular carbonyl migration coupled with imidoyl ligand rearrangement on the face of the cluster or by a carbonyl dissociation with imidoyl ligand rearrangement. We have not, as yet, differentiated between these possibilities.

Direct phosphine substitution of 3 at 100 °C also leads to the formation of **6a** and **6b** in the same ratio as that obtained from the thermolysis of 5 (eq 5).

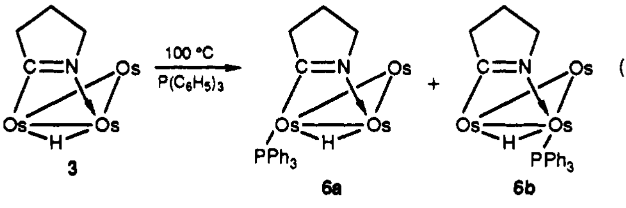

(5)

Thermolysis of 5 in octane (125 °C) for 9 h or of **6a** and **6b** in octane for 7 h yielded the same single product whose ^1H NMR, infrared, and elemental analysis are consistent with its formulation as $(\mu\text{-H})(\mu_3\text{-}\eta^2\text{-}\overline{C{=}NCH_2CH_2CH_2})\text{-}Os_3(CO)_8P(C_6H_5)_3$ (7, eq 6). We were unable to obtain

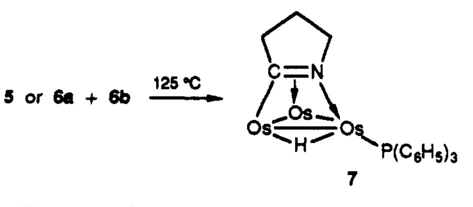

(6)

X-ray quality crystals of 7; so it is not possible to determine whether the phosphine is substituted at the carbon- or nitrogen-bound metal atom. The natural abundance proton-decoupled ^{13}C NMR spectrum of 7 in the carbonyl region at room temperature shows resonances at 172.6,

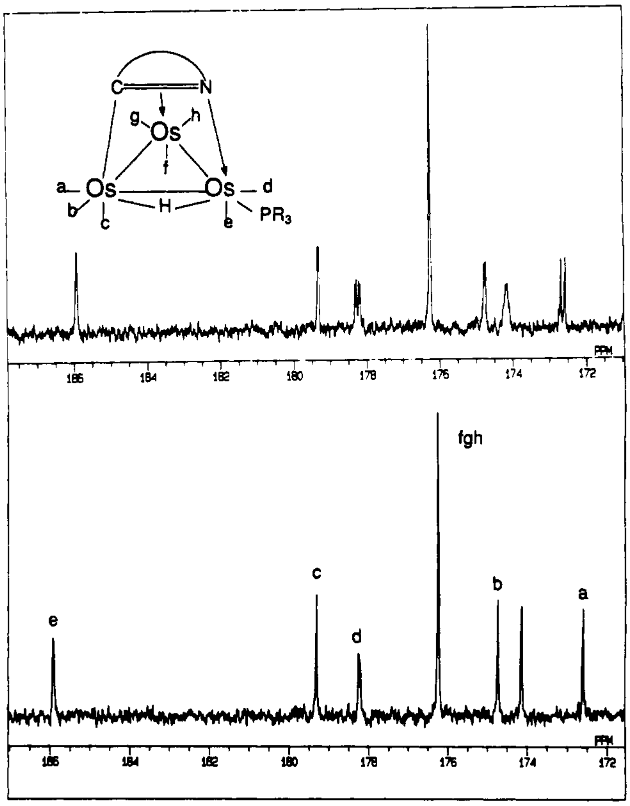

Figure 3. ^{13}C NMR of the carbonyl region of 7 at 100 MHz; proton coupled (top), proton decoupled (bottom). Assignments shown assume substitution under the nitrogen of the imidoyl ligand as for 9 (see text).

174.8, 176.2, 178.2 (J_{P-C} = 4.2 Hz), 179.4, and 185.9 ($^2J_{P-C}$ ~ 2 Hz) ppm in a relative intensity of 1:1:3:1:1:1 (Figure 3). We can assign the resonance of relative intensity three to the average of the three carbonyls on the unbridged osmium atom, which are apparently undergoing trigonal twist motion that is rapid on the NMR time scale as for 5 and related ruthenium complexes.[13] The proton-coupled ^{13}C NMR reveals hydride coupling to the resonances at 172.6 ($^2J_{H-C}$ = 12.2 Hz), 174.8 ($^2J_{H-C}$ = 4.6 Hz), 178.2 ($^2J_{H-C}$ = 10.3 Hz), and 179.3 ($^2J_{H-C}$ = 3.0 Hz) ppm. Taken together these data show conclusively that the resonance of relative intensity three at 176.2 ppm is due to the average of three carbonyls on the osmium atom not bridged by the hydride and allow us to tentatively assign all the resonances (Figure 3). A resonance of relative intensity one appears at 174.1 ppm, which is severely broadened in the proton-coupled spectrum. This resonance can be assigned to the imidoyl carbon on the basis that it would be expected to be broadened by small three-bond couplings to the adjacent methylene hydrogens. The observation of five sharp ^{13}C resonances for the remaining five carbonyls including two resolvable carbon–phosphorus two-bond couplings shows that in this μ_3-η^2-imidoyl complex the organic ligand is rigid on the NMR time scale, unlike 1, which exhibits a "windshield wiper" motion that is rapid on the NMR time scale at room temperature.[8] Substitution of phosphine for carbonyl apparently has a significant influence on the energy barrier to this process.

The reaction of 2 with triphenylphosphine at room temperature also leads to the gradual conversion to a phosphine addition product over a 24-h period. After purification an 80% yield of $(\mu\text{-H})(\mu\text{-}\eta^2\text{-}CH_3CH_2C{=}$

---

(13) Aime, S.; Gobetto, R.; Padovan, F.; Botta, M.; Rosenberg, E.; Gellert, R. W. *Organometallics* **1987**, *6*, 2074.

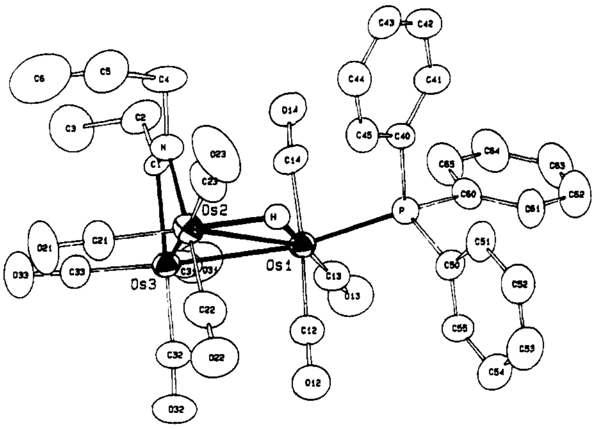

Figure 4. ORTEP drawing of $(\mu\text{-H})(\mu\text{-}\eta^2\text{-}CH_3CH_2C{=}NCH_2CH_2CH_3)Os_3(CO)_9P(C_6H_5)_3$ (**8a**) showing the calculated position of the hydride.

Table IV. Selected Bond Distances and Angles for $(\mu\text{-H})(\mu\text{-}\eta^2\text{-}CH_3CH_2C{=}NCH_2CH_2CH_3)Os_3(CO)_9P(C_6H_5)_3$ (8a)[a]

atom 1	atom 2	dist, Å	atom 1	atom 2	dist, Å
Os1	Os2	3.0559 (6)	N	C1	1.25 (1)
Os1	Os3	2.8979 (4)	C1	C2	1.53 (1)
Os2	Os3	2.7520 (5)	C2	C3	1.57 (1)
Os2	N	2.126 (9)	N	C4	1.53 (1)
Os3	C1	2.121 (9)	C4	C5	1.52 (2)
Os1	H	1.85	C5	C6	1.63 (2)
Os2	H	1.85	C	O(CO)	1.15 (1)[b]
Os1	P	2.369 (2)	C	C(Ph)	1.40 (2)[b]
Os	C(CO)	1.90 (2)[b]	P	C(Ph)	1.84 (2)[b]

atom 1	atom 2	atom 3	angle, deg	atom 1	atom 2	atom 3	angle, deg
Os1	Os2	Os3	59.59 (1)	Os1	P	C40	112.4 (2)
Os1	Os3	Os2	65.43 (1)	Os1	P	C50	117.7 (3)
Os2	Os1	Os3	54.98 (1)	Os1	P	C60	114.7 (2)
C1	N	C4	126.1 (9)	C40	P	C50	104.1 (3)
N	C1	C2	123.3 (8)	C40	P	C60	104.3 (5)
C1	C2	C3	110 (1)	C50	P	C60	102.0 (4)
N	C4	C5	110 (1)	Os	C	O(CO)	177 (1)[b]
C4	C5	C6	110 (1)	C	C	C(Ph)	120 (1)[b]

[a] Numbers in parentheses are estimated standard deviations in the least significant digits. [b] Average values.

$NCH_2CH_2CH_3)Os_3(CO)_9P(C_6H_5)_3$ (**8a**). The room temperature ^1H NMR of **8** revealed the presence of a relatively complex mixture of isomers (vide infra), in sharp contrast to **5**. We, therefore, undertook an X-ray crystallographic investigation of **8** to see if the isomer that crystallized was isostructural with **5**. The solid-state structure of **8** is illustrated in Figure 4, selected distances and bond angles are given in Table IV, and crystal data are shown in Table I. The structure of **8** consists of an osmium triangle with three distinctly different metal–metal bond lengths: Os(1)–Os(2) = 3.056 (1) Å, Os(1)–Os(3) = 2.898 (1) Å, and Os(2)–Os(3) = 2.752 (1) Å. Unlike **3** and **5** the hydride ligand in **8** does not share the same edge as the μ-imidoyl ligand. The hydride ligand was located by using the program Hydex[12] and its calculated position corroborated by the dispositions of CO(13) and CO(21), which are directly trans to the hydride, a virtually identical situation with that found for the analogues of **8** (i.e., **1**, **3**, **5**, **6**, and analogous ruthenium complexes).[8,13,14] It is significant that the hydride is bridging the osmium atom bound to nitrogen, which is in turn bound to the more bulky *n*-propyl group, rather than the osmium atom bound to carbon. We suggest that this location of the hydride, which results in considerable elongation of the Os(1)–Os(2) bond, leads to less steric crowding between the phosphine (which consistently prefers a cis orientation relative to a bridging hydride for steric reasons[9a] as observed here) and the more bulky *n*-propylalkyl side chain. Consistent with this steric argument is the fact that the Os(2)–N bond is significantly longer in **8** (2.13 (1) Å) than in **5** (2.09 (1) Å), while the stereochemical relationship between the phosphine and the nitrogen atom is the same in both complexes.

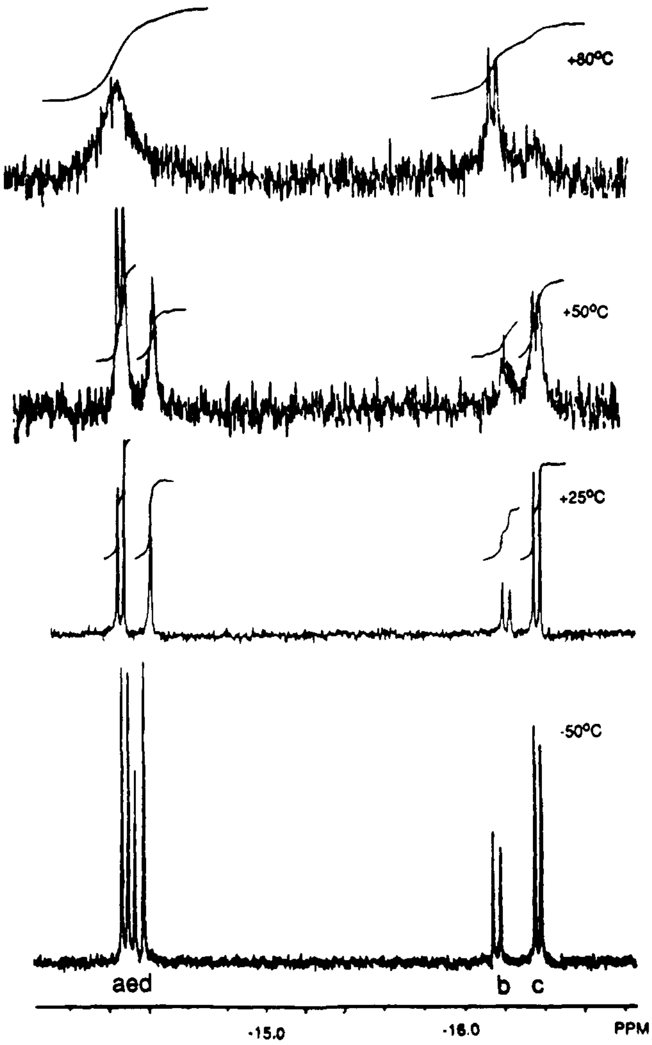

Figure 5. VT-^1H NMR spectra of compound **8** in toluene-d_8, in the hydride region at 400 MHz.

With the solid-state structure of **8** in hand we can now turn our attention to the interpretation of the ^1H NMR data. A low-temperature limiting ^1H NMR spectrum for **8** at 400 MHz in toluene-d_8 is obtained at -50 °C and the hydride region exhibits five resonances at -14.28 (d, $^2J_{P\text{-}H}$ = 12.8 Hz), -14.33 (s), -14.38 (s), -16.16 (d, $^2J_{P\text{-}H}$ = 14.8 Hz), and -16.37 (d, $^2J_{P\text{-}H}$ = 12.6 Hz) ppm with relative intensities of 3:1:1.5:1.3:2.3 (Figure 5). As the temperature is increased to +25 °C, the singlet resonances at -14.33 and -14.38 ppm average to a slightly broadened singlet at a -14.40 ppm, while the three doublet resonances remain sharp. Increasing the temperature to +50 °C leads to significant broadening of the doublet resonances. At +80 °C we observe broadening of the singlet resonance at -14.40 and the doublet at -14.28 ppm and broadening of the two upfield doublets at -16.16 and -16.37 ppm. The ^1H NMR of a separate sample of **8** at 80 MHz at 115 °C revealed that all the hydride resonances average to a

---

(14) Day, M.; Hajela, S.; Hardcastle, K. I.; McPhillips, T.; Rosenberg, E.; Botta, M.; Gobetto, R.; Milone, L.; Osella, D.; Gellert, R. W. *Organometallics* 1990, *9*, 913.

Scheme II

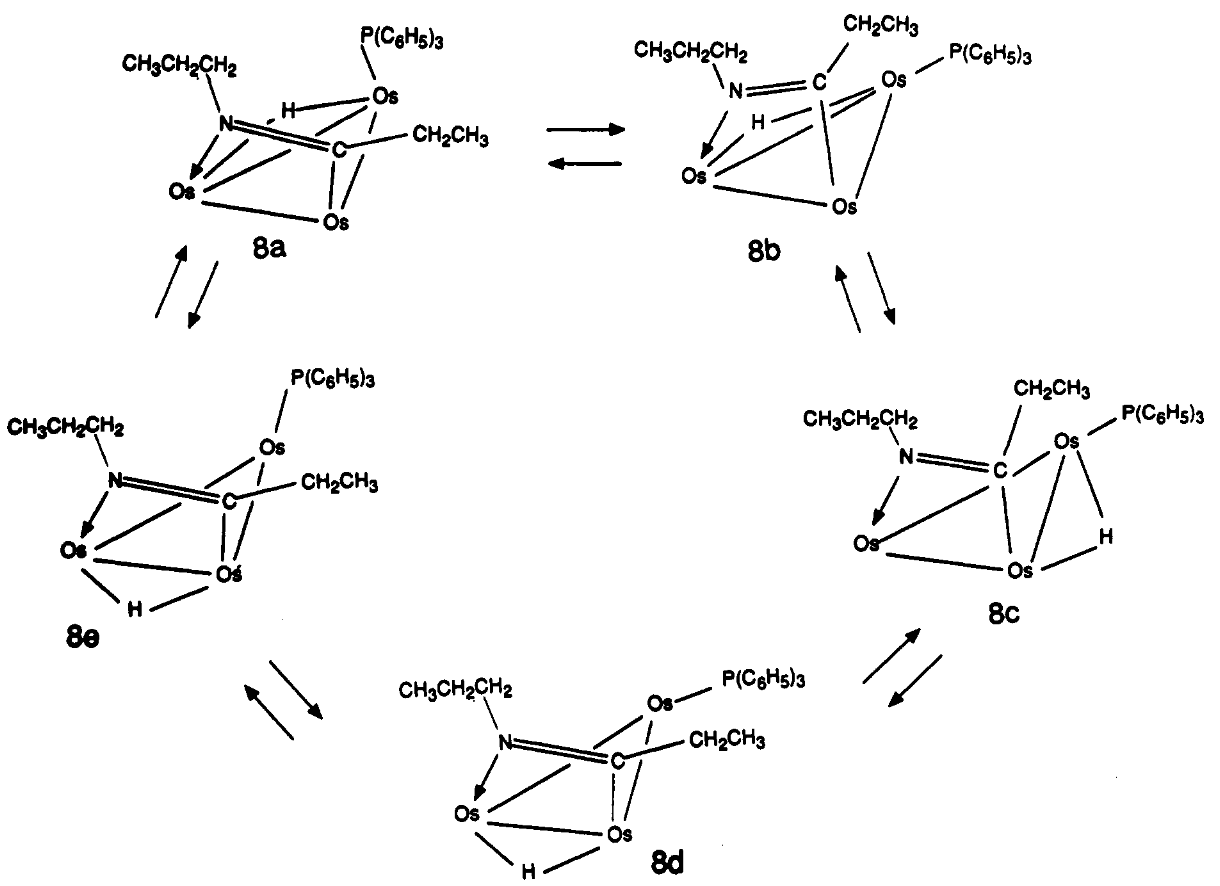

broadened doublet at −15.07 ppm.

Utilizing the solid-state structure of 8 and the variable-temperature ^{1}H NMR data we can tentatively make structural assignments to the five observed isomers (Scheme II). The major isomer, which gives rise to the doublet hydride rsonance at −14.28 ppm, should have the same structure as that observed in the solid state with the phosphine ligand cis to the hydride and syn to the nitrogen atom of the imidoyl ligand (**8a**, Scheme II). Since the size of the phosphorus–hydrogen coupling constant should be very sensitive to the dihedral angle between the Os–Os–H and Os–Os–P planes, we assign the resonance at −16.37 ppm to an isomer that has the same stereochemical relationship to the phosphine as **8a**, on the basis of their almost identical phosphorus–hydrogen coupling constants (**8c**, Scheme II), but where the phosphine and hydride are syn to the carbon of the imidoyl ligand. The third doublet resonance at −16.16 ppm, which shows a significantly larger phosphorus–hydrogen coupling (14.8 Hz), can be assigned to one of the two isomers in which the phosphine is trans to the hydride and either syn or anti to the nitrogen of the imidoyl. We suggest that the observed isomer is the one in which the phosphine is syn to the carbon of the imidoyl ligand and the hydride is syn to the nitrogen (**8b**, Scheme II) on the basis of the similarity in hydride chemical shift between **8b** and **8c** and because having the phosphine syn to the shorter alkyl group when it is cisoid to a shorter metal–metal bond (i.e., trans to the hydride) should lead to less steric crowding. The two singlet resonances at −14.33 and −14.38 ppm can be assigned to **8c** and **8d** (Scheme II), respectively, where the hydride and the imidoyl ligand share the same edge of the metal triangle and the phosphine is on the unbridged metal atom (as in **5**) on the basis of their unresolved phosphorus–hydrogen coupling constants. We can further suggest that **8d** is the more abundant of these on the basis of the same steric argument made for **8b**. Isomers **8d** and **8e** exchange with each other more rapidly than with **8a–c** as would be expected, since only a trigonal twist at one osmium atom and no hydride migration are required. We have previously shown that axial–radial ligand exchange at metal atoms not bridged by hydrogen is significantly more rapid than axial–radial exchange at hydride-bridged metal atoms in the same cluster.[15] The averaged resonance observed at +21 °C for **8d** and **8e** is shifted upfield by 0.04 to −14.40 ppm, compared with calculated average of 14.36 ppm after correcting for population changes with temperature. This upfield shift could be due to contributions to the averaged chemical shift from the axial conformer, which might be expected to have a very different chemical shift from the two radial isomers. A similar effect was seen with **5**, where the averaged signal is shifted downfield. The higher energy exchange process, which interconverts **8a–e**, must involve hydride migration but cannot involve motion of the organic ligand unless one allows for intramolecular carbonyl migration or carbonyl dissociation.

The reaction of **4** with triphenylphosphine proceeds only at 100 °C to give **8** in 66% yield and the solution ^{1}H NMR gives exactly the same distribution of isomers. This is in sharp contrast to reactions of **1** and **3** with triphenylphosphine at 25 and 100 °C, respectively, where distinctly different products are obtained and where the phosphine addition product **5** converts to **6a** and **6b** only at elevated temperatures. It would appear that the large number of isomers obtained for **8** at room temperature from **2** and at 100 °C from **4** are the result of the unusually high steric perturbations brought about by the simultaneous presence

---

[15] Barner-Thorsen, C.; Hardcastle, K. I.; Rosenberg, E.; Siegel, J.; Landfredi, A. M. M.; Tiripicchio, A.; Camellini, M. T. *Inorg. Chem.* **1981**, *20*, 4306. Rosenberg, E.; Milone, L.; Aime, S. *Inorg. Chim. Acta* **1975**, *15*, 53.

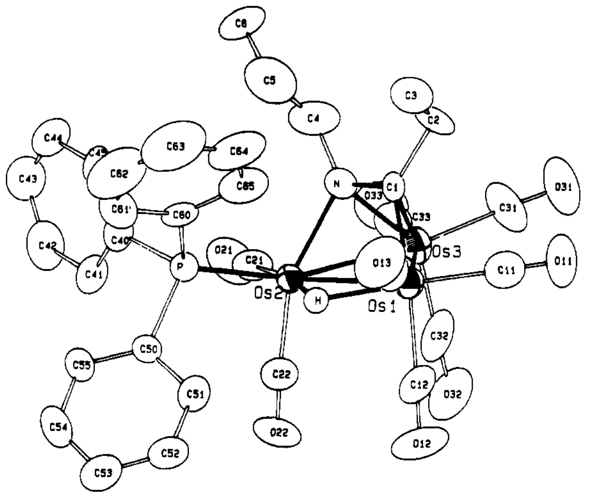

Figure 6. ORTEP drawing of $(\mu\text{-H})(\mu_3\text{-}\eta^2\text{-CH}_3\text{CH}_2\text{C}{=}\text{NCH}_2\text{CH}_2\text{CH}_3)\text{Os}_3(\text{CO})_8\text{P}(\text{C}_6\text{H}_5)_3$ showing the calculated position of the hydride ligand.

of the acyclic imidoyl ligand and of the bulky triphenylphosphine ligand.

Further thermolysis of 8 at 125 °C for 3.5 h leads to the formation of $(\mu\text{-H})(\mu_3\text{-}\eta^2\text{-CH}_3\text{CH}_2\text{C}{=}\text{NCH}_2\text{CH}_2\text{CH}_3)\text{Os}_3(\text{CO})_8\text{P}(\text{C}_6\text{H}_5)_3$ (9) in 85% yield and $(\mu\text{-H})_2(\mu\text{-}\eta^2\text{-CH}_3\text{CH}_2\text{C}{=}\text{NCH}_2\text{CH}_2\text{CH}_3)\text{Os}_3(\text{CO})_8(\mu\text{-}\eta^2\text{-C}_6\text{H}_5)_2\text{P}(o\text{-C}_6\text{H}_4))$ (10, eq 7) in 14% yield. The structures of 9 and

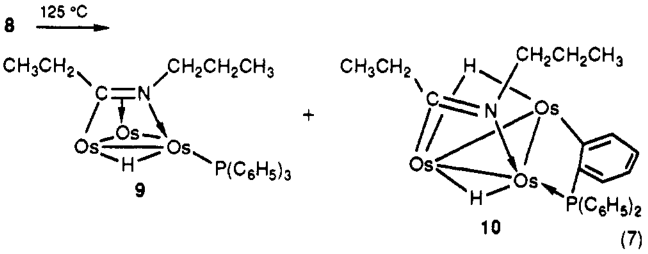

(7)

10 are based on ^{1}H NMR, infrared, and elemental analysis, with the exact locations of the phosphine, hydride, and imidoyl ligands relative to each other in 9 confirmed on the basis of a solid-state structural investigation of 9 (vide infra).

The solid-state structure of 9 is shown in Figure 6, crystal data are given in Table I, and selected distances and angles are in Table V. The solid-state structure reveals that in 9 the phosphine is on the same metal atom bound to the nitrogen of the μ_3-imidoyl ligand. Thus conversion of the imidoyl ligand from μ to μ_3 on decarbonylation, which causes the ligand to move onto the face of the cluster, provides sufficient room for the bulky triphenylphosphine under the more bulky alkyl group. Preferential location of the phosphine under nitrogen versus carbon can be rationalized on electronic grounds with the phosphines greater donor ability balanced by the more electronegative nitrogen atom. The bonding of the imidoyl ligand to the Os(1)–Os(2) edge is much more asymmetric than in 5 and 8, with Os(2)–N = 2.13 (1) Å and Os(1)–C(1) = 2.08 (1) Å in 9, while the corresponding bond lengths in 5 and 8 are within 0.01 Å of each other. The C–N bond vector in 9 is not quite parallel to the Os(1)–Os(2) edge, with the nitrogen atom about 0.01 Å closer to Os(3) than the carbon atom. This slight twisting and the asymmetry in the imidoyl ligand–metal bonding may relieve some of the steric crowding imposed on the organic ligand by the bulky phosphine. As might be expected, the C=N bond vector is considerably elongated in 9 compared with 5 or 8, being 1.37 (2) Å in 9 and 1.27 (1) and 1.25 (1) Å in 5 and 8, respectively. The same trend in C=N bond lengths was observed by Adams et al. on going from μ- to μ_3-imidoyl complexes.[6c,d] As in the previous structure the hydride was located by the program Hydex;[12] its location was corroborated by the trans disposition of CO(11) and CO(21). The μ_3 bonding of the imidoyl ligand and the relocation of the hydride ligand on the Os(1)–Os(2) edge result in considerable shortening and symmetrization of the other two metal–metal bonds in 9 relative to 5 and 8 (2.722 (1) and 2.773 (1) Å in 9; 2.912 (1) and 2.892 (1) Å in 5; 2.898 (1) and 2.752 (1) Å in 8). The similarity in the phosphorus–hydride coupling constants in 7 and 9 (14.40 and 14.65 Hz) leads us to suggest that the compounds are isostructural. These coupling constants are somewhat larger than other cisoid phosphine–hydride couplings (e.g., 6 and 8) and probably reflect an unusually small dihedral angle between the Os(1)–Os(2)–P and Os(1)–Os(2)–H planes.

Table V. Selected Bond Distances and Angles for $(\mu\text{-H})(\mu_3\text{-}\eta^2\text{-CH}_3\text{CH}_2\text{C}{=}\text{NCH}_2\text{CH}_2\text{CH}_3)\text{Os}_3(\text{CO})_8\text{P}(\text{C}_6\text{H}_5)_3$ (9)[a]

atom 1	atom 2	dist, Å	atom 1	atom 2	dist, Å
Os1	Os2	2.9332 (8)	N	C1	1.37 (2)
Os1	Os3	2.7733 (9)	N	C4	1.54 (2)
Os2	Os3	2.7222 (8)	C1	C2	1.56 (2)
Os1	C1	2.08 (1)	C2	C3	1.50 (2)
Os3	C1	2.29 (1)	C4	C5	1.32 (2)
Os2	N	2.13 (1)	C5	C6	1.55 (3)
Os3	N	2.19 (1)	Os	C(CO)	1.89 (4)[b]
Os2	P	2.357 (3)	C	O(CO)	1.14 (3)[b]
Os1	H1	1.85	C	C(Ph)	1.40 (3)[b]
Os2	H1	1.85	P	C(Ph)	1.83 (2)[b]

atom 1	atom 2	atom 3	angle, deg	atom 1	atom 2	atom 3	angle, deg
Os1	Os2	Os3	58.59 (2)	Os2	P	C40	112.8 (4)
Os1	Os3	Os2	64.51 (2)	Os2	P	C50	114.7 (4)
Os2	Os1	Os3	56.90 (2)	Os2	P	C60	118.9 (5)
N	C1	C2	120 (1)	C40	P	C50	104.2 (7)
C1	C2	C3	109 (1)	C40	P	C60	103.7 (7)
C1	N	C4	127 (1)	C50	P	C60	100.7 (5)
N	C4	C5	116 (2)	Os	C	O(CO)	177 (1)[b]
C4	C5	C6	110 (2)	C	C	C(Ph)	120 (2)[b]

[a] Numbers in parentheses are estimated standard deviations in the least significant digits. [b] Average values.

Although we were unable to obtain X-ray quality crystals of 10 the ^{1}H NMR data strongly indicate that this is an orthometallation product as indicated in eq 7. There are two hydride resonances, a doublet at −13.56 ppm ($^2J_{\text{P-H}}$ = 17.6 Hz) and a singlet at −18.78 ppm in a 1:1 ratio. The large phosphorus–hydride coupling is consistent with the phosphorus being directly trans to the hydride as would be required if the phosphine adopts the μ-η^2-orthometalated bonding mode. That the other hydride resonance is a singlet indicates that it bridges the two osmium atoms not bound to the phosphorus. The appearance of the phenyl resonances as a series of multiplets at 6.78, 6.96, 7.46, and 8.03 ppm in a relative intensity of 1:2:10:1 is also consistent with an orthometalated phenyl ring.[16-19] The fact that isolated 9 slowly converts to 10 shows that orthometalation occurs after formation of 9 and strongly suggests that the phosphine in 10 is on the nitrogen-bound osmium atom as in 9. In order for 10 to be a 48e$^-$ cluster the imidoyl ligand must be μ-η^2 not μ_3-η^2 as in 9.

---

(16) Azam, K. A.; Deeming, A. J.; Kimber, R. E.; Shukla, P. R. *J. Chem. Soc., Dalton Trans.* **1976**, 1853. Yin, C. C.; Deeming, A. J. *J. Chem. Soc., Dalton Trans.* **1974**, 1013.

(17) Ferrari, R. P.; Vaglio, G. A.; Gambino, O.; Cetini, G. *J. Chem. Soc., Dalton Trans.* **1972**, 1998.

(18) Colbran, S. B.; Irele, P. T.; Johnson, B. F. G.; Lahoz, F. J.; Lewis, J.; Ratihby, P. R. *J. Chem. Soc., Dalton Trans.* **1989**, 2023.

(19) Deeming, A. J.; Kabir, S. E.; Powerll, N. I.; Bates, P. A.; Hursthouse, B. M. *J. Chem. Soc., Dalton Trans.* **1987**, 1529.

To verify that the large number of isomers realized for **8** in solution (compared to **5**) is the result of steric crowding between the bulkier *n*-propylethyl imidoyl ligand and the triphenylphosphine, and not of some unspecified electronic factors, we reacted **2** with both $P(CH_3)_3$ and $P(OCH_3)_3$. In both cases we obtained phosphine addition products $(\mu\text{-H})(\mu\text{-}\eta^2\text{-CH}_3\text{CH}_2\text{C}{=}\text{NCH}_2\text{CH}_2\text{CH}_3)\text{Os}_3(\text{CO})_9\text{PR}_3$ (R = CH_3, **11**; R = OCH_3, **12**) whose variable-temperature ^1H NMR indicate that they are isostructural with **5**. In the case of trimethylphosphine, the low-temperature limiting ^1H NMR spectrum at −50 °C shows two singlet hydride resonances at −14.58 and −14.60 ppm in a ratio of 1:2, which average to a singlet resonance at −14.59 ppm at +50 °C. The trimethyl phosphite complex **12** shows two doublets in the hydride region at −14.95 ($^3J_{\text{P-H}} = 3.1$ Hz) and −15.00 ($^3J_{\text{P-H}} = 2.4$ Hz) ppm in a 1.2:1 ratio at 0 °C, which coalesce to a broadened singlet at −14.94 ppm at +50 °C. There is considerable precedent in the literature for the observation of small (1–3 Hz) phosphorus–hydride three-bond couplings in metal clusters.[18,20] Thus the dynamic behavior of **11** and **12** and the number of isomers observed are directly analogous to that observed for **5**. However, the populations of the isomers and the magnitude of the phosphorus–hydride couplings are somewhat sensitive to the particular phosphorous ligand.

Conclusions

The room temperature ligand addition reactions exhibited by **1** and **2** can best be described as a partial displacement of the imidoyl ligand, which goes from a $5e^-$ donor to a $3e^-$ donor on forming **5** and **8**. Although there is precedent for similar ligand additions by partial polydentate ligand displacement,[7b] it is not clear in the present case whether initial attack by the incoming ligand is at nitrogen, followed by rearrangement of the imidoyl ligand, or simply by direct displacement of the C=N π-bond. Low-temperature kinetic studies are currently under way in our laboratories to investigate this point further. There is also some precedent for the migration of a hydride from one edge of a metal cluster triangle to another occurring on phosphine substitution as observed in **2** going to **8**.[21] However, in the previously reported cases, this migration was thought to arise from electronic factors, whereas the results obtained for **2** reacting with various phosphorous ligands indicate that the products obtained arise as a result of steric factors (i.e., steric crowding between triphenylphosphine and the alkyl groups on the imidoyl ligand). The thermal rearrangement of **5** to **6a** and **6b** requires formal cleavage of the carbon–metal and carbon–nitrogen bonds if one excludes the possibility of phosphine dissociation–association, which means that the imidoyl ligand can migrate over the face of the cluster at elevated temperature in addition to the windshield wiper motion previously reported.[8] The rearrangement of **5** to **6a** and **6b** also requires a metal to metal carbonyl migration, which could occur intramolecularly or by carbonyl dissociation–association. The possible role of phosphine and carbonyl dissociation in the observed rearrangements in **5** and **8** is currently being investigated with suitable phosphine- and ^{13}CO-exchange experiments. Overall the class of relatively reactive clusters represented by **1** and **2** will afford the opportunity to gain a better understanding of the factors influencing isomer stability in metal clusters and the role of ligand dynamics in their kinetic lability.

Experimental Section

General Methods. Although the reaction products are air stable, all reactions were performed under an atmosphere of prepurified nitrogen. Reagent grade solvents were dried over molecular sieves and degassed by purging with nitrogen prior to use. Triphenylphosphine, trimethylphosphine, and trimethyl phosphite were purchased from Aldrich and used as received. The clusters $(\mu\text{-H})(\mu_3\text{-}\eta^2\text{-}\overline{\text{C}{=}\text{NCH}_2\text{CH}_2\text{C}}\text{H}_2)\text{Os}_3(\text{CO})_9$ (**1**), $(\mu\text{-H})(\mu\text{-}\eta^2\text{-}\overline{\text{C}{=}\text{NCH}_2\text{CH}_2\text{C}}\text{H}_2)\text{Os}_3(\text{CO})_{10}$ (**3**), $(\mu\text{-H})(\mu_3\text{-}\eta^2\text{-CH}_3\text{CH}_2\text{C}{=}\text{NCH}_2\text{CH}_2\text{CH}_3)\text{Os}_3(\text{CO})_9$ (**2**), and $(\mu\text{-H})(\mu\text{-}\eta^2\text{-CH}_3\text{CH}_2\text{C}{=}\text{NCH}_2\text{CH}_2\text{CH}_3)\text{Os}_3(\text{CO})_{10}$ (**4**) were prepared by published procedures.[8a] ^1H NMR spectra were obtained on an IBM-NR80, a JOEL-GX270/89, or a Bruker AM400 spectrometer. ^{13}C NMR spectra were obtained at 100 MHz on a JEOL-EX400 spectrometer. Infrared spectra were recorded on a Perkin-Elmer 1400 spectrophotometer. Elemental analyses were performed by Schwarzkopf Analytical Laboratory, New York.

Reaction of $(\mu\text{-H})(\mu_3\text{-}\eta^2\text{-}\overline{\text{C}{=}\text{NCH}_2\text{CH}_2\text{C}}\text{H}_2)\text{Os}_3(\text{CO})_9$ (1) with $P(C_6H_5)_3$. The cluster $(\mu\text{-H})(\mu_3\text{-}\eta^2\text{-}\overline{\text{C}{=}\text{NCH}_2\text{CH}_2\text{C}}\text{H}_2)\text{Os}_3(\text{CO})_9$ (**1**) (0.021 g, 0.025 mmol), $P(C_6H_5)_3$ (0.019 g, 0.072 mmol), and cyclohexane (20 mL) were combined in a flame-dried Schlenk tube and allowed to stir at room temperature for 24 h. The solvent was evaporated, and the residue was chromatographed on silica TLC plates eluting with hexane/CH_2Cl_2 (10:3, v/v) to give two bands. The top band gave unreacted $(\mu\text{-H})(\mu_3\text{-}\eta^2\text{-}\overline{\text{C}{=}\text{NCH}_2\text{CH}_2\text{C}}\text{H}_2)\text{Os}_3(\text{CO})_9$ (0.001 g), while the second band afforded $(\mu\text{-H})(\mu\text{-}\eta^2\text{-}\overline{\text{C}{=}\text{NCH}_2\text{CH}_2\text{C}}\text{H}_2)\text{Os}_3(\text{CO})_9\text{P}(\text{C}_6\text{H}_5)_3$ (**5**) (0.025 g, 93%) as yellow crystals after recrystallization from hexane/CH_2Cl_2.

Analytical Data for 5. Anal. Calcd for $C_{31}H_{22}NO_9POs_3$: C, 32.26; H, 1.93; N, 1.21. Found: C, 32.41; H, 1.81; N, 1.24. IR (CH_2Cl_2, ν_{CO}): 2046 s, 2011 m, 1196 sh, 1992 s, 1971 br, 1944 br cm^{-1}. 400-MHz ^1H NMR ($CDCl_3$, −50 °C): major isomer (~66%) 7.50 (m, 15 H), 3.42 (m, 2 H), 2.33 (m, 2 H), 1.43 (m, 2 H), −15.08 (s, 1 H) ppm; minor isomer (~33%) 7.50 (m, 15 H), 3.42 (m, 2 H), 2.33 (m, 2 H), 1.43 (m, 2 H), −15.01 ppm.

Conversion of 5 to 6. Compound **5** (0.017 g, 0.015 mmol) in heptane (20 mL) was heated to reflux under nitrogen for 16 h, during which time IR analysis indicated complete reaction. The solvent was removed by rotary evaporation and the residue was chromatographed on silica TLC plates to give two bands, which afforded clusters **6** (0.013 g, 76%) and **5** (0.002 g) in order of elution.

Analytical Data for 6. Anal. Calcd for $C_{31}H_{22}NO_9POs_3$: C, 32.26; H, 1.93; N, 1.21. Found: C, 32.19; H, 1.78; N, 1.23. IR (ν_{CO}, CH_2Cl_2): 2084 s, 2043 vs, 2004 vs, 1990 s, 1969 m, 1935 w cm^{-1}. 80-MHz ^1H NMR (CD_2Cl_2): major isomer (80%) 7.44 (m, 15 H), 3.48 (m, 2 H), 2.15–0.88 (m, 4 H), −14.76 (d, 1 H, $J_{\text{P-H}} = 9.9$ Hz) ppm; minor isomer (20%) 7.44 (m, 15 H), 3.48 (m, 2 H), 2.15–0.88 (m, 4 H), −14.81 (d, 1 H, $J_{\text{P-H}} = 10.0$ Hz) ppm.

Reaction of $(\mu\text{-H})(\mu\text{-}\eta^2\text{-}\overline{\text{C}{=}\text{NCH}_2\text{CH}_2\text{C}}\text{H}_2)\text{Os}_3(\text{CO})_{10}$ (3) with $P(C_6H_5)_3$. To a solution of $(\mu\text{-H})(\mu\text{-}\eta^2\text{-}\overline{\text{C}{=}\text{NCH}_2\text{CH}_2\text{C}}\text{H}_2)\text{Os}_3(\text{CO})_{10}$ (0.083 g, 0.090 mmol) in heptane (25 mL) in a flame-dried Schlenk tube was added $P(C_6H_5)_3$ (0.030 g, 0.114 mmol) and the reaction mixture was heated to reflux under nitrogen for 13 h. The solvent was rotary evaporated and the residue was chromatographed on silica TLC plates eluting with hexane/CH_2Cl_2 (10:3, v/v) to resolve two bands. The first band gave unreacted $(\mu\text{-H})(\mu\text{-}\eta^2\text{-}\overline{\text{C}{=}\text{NCH}_2\text{CH}_2\text{C}}\text{H}_2)\text{Os}_3(\text{CO})_{10}$ (**3**) (0.052 g) and the second band gave $(\mu\text{-H})(\mu\text{-}\eta^2\text{-}\overline{\text{C}{=}\text{NCH}_2\text{CH}_2\text{C}}\text{H}_2)\text{Os}_3(\text{CO})_9\text{P}(\text{C}_6\text{H}_5)_3$ (**6**) (0.033 g, 80% based on consumed **3**) as orange crystals after recrystallization from hexane/CH_2Cl_2.

Thermolysis of $(\mu\text{-H})(\mu\text{-}\eta^2\text{-}\overline{\text{C}{=}\text{NCH}_2\text{CH}_2\text{C}}\text{H}_2)\text{Os}_3(\text{CO})_9\text{P}(\text{C}_6\text{H}_5)_3$ (6). In a three-necked round-bottom flask $(\mu\text{-H})(\mu\text{-}\eta^2\text{-}\overline{\text{C}{=}\text{NCH}_2\text{CH}_2\text{C}}\text{H}_2)\text{Os}_3(\text{CO})_9\text{P}(\text{C}_6\text{H}_5)_3$ (**6**) (0.034 g, 0.029 mmol) and 20 mL of octane were combined. The reaction mixture was refluxed under nitrogen for 7 h, rotary evaporated, taken up in methylene chloride, and chromatographed on silica TLC plates

---

[20] (a) Jangala, C.; Rosenberg, E.; Skinner, D.; Aime, S.; Milone, L.; Sappa, E. *Inorg. Chem.* **1980**, *19*, 1571. (b) Ditzel, E. J.; Johnson, B. F. G.; Lewis, J. *J. Chem. Soc., Dalton Trans.* **1987**, 1289.

[21] Adams, R. D.; Selegue, J. P. *Abstr. Am. Crystallogr. Assoc.* **1980**, 28.

eluting with hexane/CH_2Cl_2 (10:3, v/v) to resolve two bands. The first band gave unreacted **6** (0.001 g) and the second band gave $(\mu\text{-H})(\mu_3\text{-}\eta^2\text{-}\overline{\text{C}{=}\text{NCH}_2\text{CH}_2\text{C}}\text{H}_2)\text{Os}_3(\text{CO})_8\text{P}(\text{C}_6\text{H}_5)_3$ (**7**) (0.030 g, 91%) as yellow crystals after recrystallization from hexane/CH_2Cl_2.

Analytical Data for 7. Anal. Calcd for $C_{30}H_{22}NO_8POs_3$: C, 32.0; H, 1.97; N, 1.24. Found: C, 32.19; H, 2.00; N, 1.18. IR (hexane, ν_{CO}): 2070 m, 2035 s, 2005 s, 1997 w, 1977 w, 1967 w, 1956 w, 1943 vw cm^{-1}. 270-MHz ^{1}H NMR ($CDCl_3$): 7.45 (m, 15 H), 3.06 (m, 1 H), 2.67 (m, 2 H), 1.67 (m, 1 H), 1.25 (m, 2 H), −17.30 (d, 1 H, J_{P-H} = 14.4 Hz) ppm. Natural abundance proton-decoupled ^{13}C NMR ($CDCl_3$): 172.6 (s), 174.8 (s), 176.2 (s), 178.2 (d, $^2J_{P-C}$ = 4.2 Hz), 179.4 (s), 185.9 (d, $^2J_{P-C} \sim 2$ Hz) ppm, in a relative intensity ratio of 1:1:3:1:1:1.

Thermolysis of $(\mu\text{-H})(\mu\text{-}\eta^2\text{-}\overline{\text{C}{=}\text{NCH}_2\text{CH}_2\text{C}}\text{H}_2)\text{Os}_3(\text{CO})_9\text{P}(\text{C}_6\text{H}_5)_3$ (5). A similar thermolysis of **5** (0.034 g, 0.019 mmol) to that above for **6** in octane for 9 h, followed by similar chromatographic workup, gave **7** (0.024 g, 73%) as yellow crystals after recrystallization from hexane/CH_2Cl_2.

Reaction of $(\mu\text{-H})(\mu_3\text{-}\eta^2\text{-CH}_3\text{CH}_2\text{C}{=}\text{NCH}_2\text{CH}_2\text{CH}_3)\text{Os}_3(\text{CO})_9$ (2) with $P(C_6H_5)_3$. $P(C_6H_5)_3$ (0.072 g, 0.274 mmol) was added to a cyclohexane solution (25 mL) of **2** (0.126 g, 0.137 mmol). This mixture was allowed to stir at room temperature for 24 h. The solvent was removed under reduced pressure and the residue was dissolved in a minimum volume of CH_2Cl_2 and applied to silica gel preparative TLC plates. Elution with hexane/CH_2Cl_2 (10:2, v/v) gave two bands. The fast moving band gave unreacted **2** (0.005 g), while the second band gave $(\mu\text{-H})(\mu\text{-}\eta^2\text{-CH}_3\text{CH}_2\text{C}{=}\text{NCH}_2\text{CH}_2\text{CH}_3)\text{Os}_3(\text{CO})_9\text{P}(\text{C}_6\text{H}_5)_3$ (**8**) as orange crystals after recrystallization from methanol/CH_2Cl_2 at −20 °C (0.130 g, 80%).

Analytical Data for 8. Anal. Calcd for $C_{33}H_{28}NO_9POs_3$: C, 33.47; H, 2.39; N, 1.18. Found: C, 33.56; H, 2.58; N, 1.25. IR (ν_{CO}, hexane): 2077 m, 2046 s, 2020 s, 1996 s, 1985 m, 1975 m, 1955 m, 1938 m cm^{-1}. 400-MHz ^{1}H NMR (toluene-d_8, −50 °C): hydride peaks that may be attributed to five isomers (**a**–**e**) were observed (isomer **a**, ~34%) −14.28 (d, 1 H, J_{P-H} = 12.8 Hz), (isomer **b**, ~14%) −16.16 (d, 1 H, J_{P-H} = 14.8 Hz), (isomer **c**, ~25%) −16.37 (1 H, J_{P-H} = 12.6 Hz), (isomer **d**, ~17%) −14.38 (s, 1 H), (isomer **e**, ~10%) −14.33 (s, 1 H) ppm. The peaks due to the methylene and methyl protons of the imidoyl ligand and phenyl protons of phosphine ligand for isomers (**a**–**e**) were not assigned due to extensive overlap; 7.67–6.85 (m, C_6H_5), 4.00 (m, CH_2), 3.44 (m, CH_2), 3.23 (m, CH_2), 2.77 (m, CH_2), 2.64 (m, CH_2), 2.52 (m, CH_2), 2.50 (m, CH_2), 2.48 (m, CH_2), 2.37 (m, CH_2), 2.29–2.10 (m, CH_2), 1.96 (m, CH_2), 1.75 (m, CH_2), 1.48 (m, CH_2), 1.0–1.36 (m, CH_2), 0.99 (t, CH_3, J_{H-H} = 7.7 Hz), 0.95 (t, CH_3, J_{H-H} = 7.4 Hz), 0.79 (t, CH_3, J_{H-H} = 7.8 Hz), 0.74 (t, CH_3, J_{H-H} = 7.6 Hz), 0.56 (t, CH_3, J_{H-H} = 7.2 Hz), 0.49 (t, CH_3, J_{H-H} = 6.9 Hz) ppm.

Reaction of $(\mu\text{-H})(\mu\text{-}\eta^2\text{-CH}_3\text{CH}_2\text{C}{=}\text{NCH}_2\text{CH}_2\text{CH}_3)\text{Os}_3(\text{CO})_{10}$ (4) with $P(C_6H_5)_3$. To a heptane solution (30 mL) of **4** (0.160 g, 0.170 mmol) in a flame-dried Schlenk tube was added $P(C_6H_5)_3$ (0.100 g, 0.381 mmol). The reaction mixture was refluxed for 2.5 h. The color changed from yellow to orange. Workup as above followed by similar chromatographic separation gave unreacted **4** (0.055 g) and **8** (0.110 g, 83% based on consumed **4**).

Thermolysis of $(\mu\text{-H})(\mu\text{-}\eta^2\text{-CH}_3\text{CH}_2\text{C}{=}\text{NCH}_2\text{CH}_2\text{CH}_3)\text{Os}_3(\text{CO})_9\text{P}(\text{C}_6\text{H}_5)_3$ (8). An octane solution (30 mL) of **8** (0.090 g, 0.076 mmol) was refluxed for 3.5 h. The solvent was removed in vacuo and the residue was chromatographed on silica TLC plates. Elution with hexane/CH_2Cl_2 (10:3, v/v) gave, in order of elution, $((\mu\text{-H})_2(\mu\text{-}\eta^2\text{-CH}_3\text{CH}_2\text{C}{=}\text{NCH}_2\text{CH}_2\text{CH}_3)\text{Os}_3(\text{CO})_8(\mu\text{-}\eta^2\text{-}(\text{C}_6\text{H}_5)_2\text{P}(o\text{-C}_6\text{H}_4))$ (**10**) (0.012 g, 14%) as pale yellow crystals after recrystallization from hexane/CH_2Cl_2 at −20 °C and $(\mu\text{-H})(\mu_3\text{-}\eta^2\text{-CH}_3\text{CH}_2\text{C}{=}\text{NCH}_2\text{CH}_2\text{CH}_3)\text{Os}_3(\text{CO})_8\text{P}(\text{C}_6\text{H}_5)_3$ (**9**) as yellow crystals after recrystallization from hexane/CH_2Cl_2 at −20 °C (0.075 g, 85%).

Analytical Data. Compound 9. Anal. Calcd for $C_{32}H_{28}NO_8POs_3$: C, 33.24; H, 2.45; N, 1.21. Found: C, 33.38; H, 2.62; N, 1.28. IR (ν_{CO}, hexane): 2069 s, 2034 vs, 2005 s, 1994 m, 1978 m, 1964 m, 1958 m, 1943 w cm^{-1}. 80-MHz ^{1}H NMR ($CDCl_3$): 7.42 (m, 15 H), 2.81 (m, 4 H), 2.34 (m, 2 H), 1.21 (t, 3 H, J_{H-H} = 7.6 Hz), 0.51 (t, 3 H, J_{H-H} = 6.4 Hz), −16.40 (d, 1 H, J_{P-H} = 14.6 Hz) ppm.

Compound 10. Anal. Calcd for $C_{32}H_{28}NO_8POs_3$: C, 33.24; H, 2.45; N, 1.21. Found: C, 33.35; H, 2.61; N, 1.26. IR (ν_{CO}, hexane): 2069 vs, 2025 s, 2017 vs, 1995 s, 1976 s, 1961 s cm^{-1}. 80-MHz ^{1}H NMR (CD_2Cl_2): 8.03 (m, 1 H), 7.46 (m, 10 H), 6.96 (m, 2 H), 6.78 (m, 1 H), 3.54–1.90 (m, 6 H), 1.38 (t, 3 H, J_{H-H} = 7.2 Hz), 0.60 (t, 3 H, J_{H-H} = 7.3 Hz), −13.56 (d, 1 H, J_{P-H} = 17.6 Hz), −18.78 (s, 1 H) ppm.

Conversion of 9 to 10. An octane solution (35 mL) of **9** (0.075 g, 0.065 mmol) was refluxed for 9 h. The solvent was removed under vacuum and the residue was chromatographed on silica gel TLC plates eluting with hexane/CH_2Cl_2 (10:3, v/v) to give two bands. The top band gave **10** (0.27 g, 60% based on consumed **9**) and the second band gave unchanged **9** (0.030 g).

Reaction of $(\mu\text{-H})(\mu_3\text{-}\eta^2\text{-CH}_3\text{CH}_2\text{C}{=}\text{NCH}_2\text{CH}_2\text{CH}_3)\text{Os}_3(\text{CO})_9$ (2) with $P(CH_3)_3$. To a cyclohexane solution (25 mL) of **2** (0.075 g, 0.081 mmol) was added $P(CH_3)_3$ (14 μL, 0.131 mmol) and the reaction mixture was allowed to stir at room temperature for 21 h. The solvent was removed under reduced pressure and the residue was chromatographed on silica gel TLC plates. Elution with a hexane/CH_2Cl_2 mixture (10:3, v/v) gave one main band from which the cluster $(\mu\text{-H})(\mu\text{-}\eta^2\text{-CH}_3\text{CH}_2\text{C}{=}\text{NCH}_2\text{CH}_2\text{CH}_3)\text{Os}_3(\text{CO})_9\text{P}(\text{CH}_3)_3$ (**11**) was isolated as yellow crystals after recrystallization from hexane/CH_2Cl_2 at −20 °C (0.081 g, 84%).

Analytical Data for 11. Anal. Calcd for $C_{18}H_{22}NO_9POs_3$: C, 21.66; H, 2.23; N, 1.40. Found: C, 21.97; H, 2.16; N, 1.43. IR (ν_{CO}, hexane): 2072 s, 2040 vs, 2010 vs, 2010 vs, 1990 vs, 1976 w, 1967 m, 1958 m, 1947 m, 1942 sh cm^{-1}. 400-MHz ^{1}H NMR ($CDCl_3$, −50 °C): major isomer (~66%) 3.55 (m, 1 H), 3.25 (m, 1 H), 2.79 (m, 1 H), 2.22 (m, 1 H), 1.88 (d, 3 H, J_{P-H} = 9.9 Hz), 1.65 (m, 2 H), 1.00 (t, 3 H, J_{H-H} = 6.8 Hz), −14.60 (s, 1 H) ppm; minor isomer (~33%) 3.84 (m, 1 H), 2.98 (m, 1 H), 2.69 (m, 1 H), 2.38 (m, 1 H), 1.88 (d, 3 H, J_{P-H} = 9.9 Hz), 1.42 (m, 2 H), 1.00 (t, 3 H, J_{H-H} = 7.8 Hz), 0.86 (t, 3 H, J_{H-H} = 6.8 Hz), −14.58 (s, 1 H) ppm.

Reaction of 2 with $P(OCH_3)_3$. A cyclohexane solution of **2** (0.099 g, 0.107 mmol) and $P(OCH_3)_3$ (19 μL, 0.161 mmol) was stirred at room temperature for 21 h at which time analytical TLC indicated complete consumption of **2**. The solvent and excess $P(OCH_3)_3$ were removed under vacuum. The residue was chromatographed on silica gel TLC plates eluting with hexane/CH_2Cl_2 (10:3, v/v). Only one major band was eluted from which the cluster $(\mu\text{-H})(\mu\text{-}\eta^2\text{-CH}_3\text{CH}_2\text{C}{=}\text{CH}_2\text{CH}_2\text{CH}_3)\text{Os}_3(\text{CO})_9\text{P}(\text{OCH}_3)_3$ (**12**) was isolated as yellow crystals after recrystallization from CH_2Cl_2/CH_3OH at −20 °C (0.107 g, 96%).

Analytical Data for 12. Anal. Calcd for $C_{18}H_{22}NO_{12}POs_3$: C, 20.67; H, 2.12; N, 1.34. Found: C, 20.85; H, 2.10; N, 1.32. IR (ν_{CO}, hexane): 2078 w, 2047 vs, 2020 m, 2010 m, 1996 vs, 1985 w, 1971 s, 1955 w cm^{-1}. 400-MHz ^{1}H NMR ($CDCl_3$, 0 °C): major isomer (~55%) 3.64 (d, 3 H, J_{P-H} = 12.2 Hz), 3.58 (m, 1 H), 3.18 (m, 1 H), 2.80 (m, 1 H), 2.16 (m, 1 H), 1.63 (m, 2 H), 1.00 (m, 3 H), 0.84 (m, 3 H) −14.95 (d, 1 H, J_{P-H} = 3.1 Hz) ppm; minor isomer (~45%) 3.79 (m, 1 H), 3.66 (d, 3 H, J_{P-H} = 12.2 Hz), 2.96 (m, 1 H), 2.67 (m, 1 H), 2.34 (m, 1 H), 1.34 (m, 2 H), 1.00 (m, 3 H), 0.84 (m, 3 H), −15.00 (d, 1 H, J_{P-H} = 2.4 Hz) ppm.

X-ray Structure Determination of 5, 6a, 8a, and 9. Crystals of **5**, **6a**, and **9** for X-ray studies were obtained from saturated solutions of each in CH_2Cl_2/hexane solvent systems at −20 °C. Suitable crystals of **8a** were obtained by recrystallization from CH_2Cl_2/CH_3OH solvent system at −20 °C. Crystals having approximate dimensions 0.03 × 0.20 × 0.10 mm for **5**, 0.38 × 0.20 × 0.15 mm for **6a**, 0.03 × 0.09 × 0.10 mm for **8a**, and 0.33 × 0.13 × 0.08 mm for **9** were examined by using similar procedures, as follows. Suitable crystals of each were mounted on glass fibers, placed in a goniometer head on an Enraf-Nonius CAD4 diffractometer, and centered optically. Unit cell parameters and an orientation matrix for data collection were obtained from 23 reflections with $8° < \theta < 16°$ for **5**, 23 reflections with $8° < \theta < 12°$ for **6a**, 23 reflections with $7° < \theta < 16°$ for **8a**, and 23 reflections with $4° < \theta < 12°$ for **9**, using the centering program in the CAD4 system. Details of crystal data are given in Table I. The lack of any systematic absences and density considerations indicated the space group $P\bar{1}$ for **5** and **8a**. Systematic absences of $h0l$, $l = 2n + 1$, and $0k0$, $k = 2n + 1$ uniquely defined the space group $P2_1/c$ for **6a**, and systematic absences of $h00$, $h = 2n + 1$, $0k0$, $k = 2n + 1$, and $00l$, $l = 2n + 1$, for **9** uniquely defined the orthorhombic space group $P2_12_12_1$. The space groups were verified by successful least-squares refinement of the structures. For each crystal the actual scan range was calculated by scan width = scan range + 0.35 tan θ and backgrounds were measured by using the moving crystal–moving counter technique, at the beginning and end of each scan. As a check on instrument and crystal stability, two representative reflections were measured every 2 h for **5**, **8a**, and **9**. Three such reflections were used in the collection of data for **6a**. Lorentz, polarization, and decay corrections were applied, as was an empirical absorption correction based on a series of ψ scans. The number of data observed and used for least-squares refinement with $F_o > 3\sigma(F_o)$ for each crystal are listed in Table I. All other reflections were considered to be unobserved.

Each of the structures was solved by the Patterson method using SHELXS-86,[22] which revealed the positions of the metal atoms. All other non-hydrogen atoms were found by successive difference Fourier syntheses. The hydride positions were calculated by using the program Hydex.[12] No other hydrogens were located. The hydride positions were included in the structure factor calculations but not refined in the final least-squares cycles. All non-hydrogen atoms were refined anisotropically. Selected bond distances and angles are given in Tables II–V and the residual electron densities in the final structures are listed in Table I.

Scattering factors were taken from Cromer and Waber.[23] Anomalous dispersion corrections were those of Cromer.[24] All calculations were carried out on a DEC MicroVax II computer, using the SDP/VAX system of programs.

Acknowledgment. We gratefully acknowledge the support of the National Science Foundation (CHE-9016495) for support of this research. We thank the NATO Science Program for a travel grant (E.R. and L.M.) and the Consiglio Nazionale delle Ricerche and the Ministero dell Universita (L.M). We also acknowledge Prof. A. Fratiello and R. Perrigan at California State University, Los Angeles, for help in obtaining 400-MHz ^{1}H NMR spectra and Johnson-Matthey for a loan of osmium tetroxide (D.O.).

Supplementary Material Available: Tables 6–9, listing atomic positions, Tables 10–13, listing anisotropic displacement factors, and Tables 14–17, listing bond distances and angles for **5**, **6a**, **8a**, and **9** (29 pages); Tables 18–21, listing calculated and observed structure factors for **5**, **6a**, **8a**, and **9** (167 pages). Ordering information is given on any current masthead page.

---

[22] Sheldrick, G. M. SHELXS-86, Program for Crystal Structure Solution, University of Gottingem, 1986.

[23] Cromer, D. T.; Waber, J. T. *International Tables for X-ray Crystallography*; Kynoch Press: Birmingham, England, 1974; Vol. IV, Table 2.2B.

[24] Cromer, D. T. *International Tables for X-ray Crystallography*; Kynoch Press: Birmingham, England, 1974; Vol. IV, Table 2.3.1.

Formation of Metallacyclic (Zirconoxycarbene)vanadium Complexes from $CpV(CO)_4$ and Their Conversion into Ordinary Fischer-Type Carbene Complexes of Vanadium

Gerhard Erker* and Ronald Pfaff

Organisch-Chemisches Institut der Universität Münster, Corrensstrasse 40, D-4400 Münster, FRG

Carl Krüger and Stefan Werner

Max-Planck-Institut für Kohlenforschung, Kaiser-Wilhelm-Platz 1, D-4330 Mülheim a.d. Ruhr, FRG

Received March 25, 1991

(*s-trans*-Butadiene)zirconocene (**8**) adds to a carbonyl ligand of $CpV(CO)_4$ to give the [(π-allyl)zirconoxycarbene]vanadium complex $Cp_2\overline{ZrOC[{=}VCp(CO)_3]C_4H_6}$ (**11b**). (butadiene)$HfCp_2$ reacts similarly to give a mixture of the [(π-allyl)hafnoxycarbene]- and seven-membered metallacyclic [(σ-allyl)hafnoxycarbene]vanadium species (**11a**/**12a**). These complexes subsequently add a ketone (acetone, acetophenone, methyl vinyl ketone), aldehyde (acrolein), or nitrile (pivalonitrile) to yield nine-membered metaloxycarbene vanadium complexes, such as $Cp_2\overline{HfOC[{=}VCp(CO)_3]CH_2CH{=}CHCH_2C(CH_3)_2O}$ (**13a**), exhibiting analogous chiral *trans*-cycloalkene dioxametalla-*trans*-cyclononene frameworks. The (carbene)vanadium complex **13a** was characterized by X-ray diffraction. Complex **13a** crystallizes in space group $P2_1/c$ with cell constants $a = 11.741$ (1) Å, $b = 14.244$ (2) Å, $c = 15.824$ (1) Å, $\beta = 109.57$ (1)°, $Z = 4$, $R = 0.028$, $R_w = 0.023$. Treatment of the nine-membered metaloxycarbene complexes with tetrabutylammonium fluoride trihydrate in tetrahydrofuran solution gave the Zr,Hf-free vanadium acylmetalate complexes $[Cp(CO)_3V({=}O)CH_2CH{=}CHCH_2CR^1R^2OH](NBu_4)$, which were subsequently O-alkylated with triethyloxonium tetrafluoroborate to yield the ordinary Fischer-type (carbene)vanadium complexes $Cp(CO)_3V{=}C(OC_2H_5)CH_2CH{=}CHCH_2CR^1R^2OH$. Treatment of $Cp_2\overline{ZrOC[{=}VCp(CO)_3]C_4H_6}$ (**11b**) with TBAF·$3H_2O$ followed by the reaction with Meerwein's reagent gave $Cp(CO)_3V{=}C(OC_2H_5)CH_2CH{=}CHCH_3$ (**24**).

Heteroatom-stabilized carbene complexes play an important role as stoichiometric reagents in organic synthesis. They are becoming increasingly important as catalysts for the selective conversion of unsaturated organic substrates.[1] Carbene complexes are readily available for most transition metals. However, there are a few situations where carbene complexes of neither the Fischer nor the Schrock type seem to be obtained easily. Among others, this applies for the d-block element vanadium. To our knowledge only a very limited number of heteroatom-stabilized (carbene)vanadium complexes have been mentioned in the literature. So far, notable examples are complexes **3** and **5**,[2] both of which were prepared by synthetic routes avoiding the

---

[1] See, e.g.: Casey, C. P. In *Transition Metal Organometallics in Organic Synthesis*; Alper, H., Ed.; Academic Press: New York, 1976; Vol. 1, p 190. Brown, F. J. *Prog. Inorg. Chem.* **1980**, *27*, 1. Dötz, K. H. *Angew. Chem.* **1984**, *96*, 573; *Angew. Chem., Int. Ed. Engl.* **1984**, *23*, 587. Schubert, U.; Fischer, H.; Hofmann, P.; Weiss, K.; Dötz, K. H.; Kreissl, F. R. *Transition Metal Carbene Complexes*; Verlag Chemie: Weinheim, Germany, 1983.

[2] Hartshorn, A. J.; Lappert, M. F.; Turner, K. *J. Chem. Soc., Dalton Trans.* **1978**, 348. Martin, J.; Moise, C.; Tirouflet, J. *C. R. Hebd. Seances Acad. Sci., Ser. 2* **1981**, *292*, 1143.

0276-7333/91/2310-3559$02.50/0